Amino Acids (2014) 46:1047–1058
DOI 10.1007/s00726-013-1661-3

ORIGINAL ARTICLE

A BODIPY-embedding miltefosine analog linked to cell-penetrating Tat(48-60) peptide favors intracellular delivery and visualization of the antiparasitic drug

Beatriz G. de la Torre · Valentín Hornillos · Juan R. Luque-Ortega · M. A. Abengózar · Francisco Amat-Guerri · A. Ulises Acuña · Luis Rivas · David Andreu

Received: 24 July 2013 / Accepted: 29 December 2013 / Published online: 21 January 2014

Abstract Therapeutic application of many drugs is often hampered by poor or denied access to intracellular targets. A case in point is miltefosine (MT), an orally active antiparasitic drug, which becomes ineffective when parasites develop dysfunctional uptake systems. We report here the synthesis of a fluorescent BODIPY-embedding MT analogue with appropriate thiol functionalization allowing linkage to the cell-penetrating Tat(48-60) peptide through disulfide or thioether linkages. The resulting constructs are efficiently internalized into the otherwise MT-invulnerable R40 *Leishmania* strain, resulting in fast parasite killing, and hence successful avoidance of the resistance. In the disulfide-linked conjugate, an additional fluoro tag on the Tat moiety allows to monitor its reductive cleavage within the cytoplasm. Terminally differentiated cells such as peritoneal macrophages, impervious to MT unless infected by *Leishmania,* can uptake the drug in its Tat-conjugated form. The results afford proof-of-principle for using CPP vectors to avert drug resistance in parasites, and/or for tackling leishmaniasis by modulating macrophage uptake.

Keywords BODIPY · Cell-penetrating peptide · Miltefosine · Dual fluorescent labeling · Reversion of resistance · Monitoring of intracellular drug delivery

Abbreviations

Boc	Tert-Butyloxycarbonyl
BDP	BODIPY: 4,4-difluoro-4-bora-3a,4a-diaza-s-indacene
CPP	Cell-penetrating peptide
DIEA	Diisopropylethylamine
DIPCI	Diisopropylcarbodiimide
Fmoc	9-Fluorenylmethyloxycarbonyl
HBTU	2-(1H-Benzotriazol-1-yl)-1,1,3,3-tetramethyluronium hexafluorophosphate
Mmt	4-Methoxytrityl
MT	Miltefosine: hexadecylphosphocholine
Npys	3-Nitro-2-pyridylsulfenyl
TFA	Trifluoroacetic acid
TIS	Triisopropylsilane

Introduction

Poor intracellular accumulation accounts for the failure of not a few drugs (Martinez and Amidon 2002). Low

Dedicated to the memory of Prof. Francisco Amat-Guerri, who passed away during the preparation of this article.

B. G. de la Torre and V. Hornillos contributed equally to this work.

Electronic supplementary material The online version of this article (doi:10.1007/s00726-013-1661-3) contains supplementary material, which is available to authorized users.

B. G. de la Torre · D. Andreu (✉)
Department of Experimental and Health Sciences, Pompeu Fabra University, Barcelona Biomedical Research Park, 08003 Barcelona, Spain
e-mail: david.andreu@upf.edu

V. Hornillos · F. Amat-Guerri
Instituto de Química Orgánica General, CSIC, Juan de la Cierva 3, 28006 Madrid, Spain

V. Hornillos · A. Ulises Acuña
Instituto de Química Física "Rocasolano", CSIC, Serrano 119, 28006 Madrid, Spain

J. R. Luque-Ortega · M. A. Abengózar · L. Rivas (✉)
Centro de Investigaciones Biológicas, CSIC, Ramiro de Maeztu 9, 28040 Madrid, Spain
e-mail: luis.rivas@cib.csic.es

internalization levels may simply reflect low affinity of the drug for cellular membranes (e.g., drugs too hydrophilic to traverse a lipid bilayer), but often faulty drug accumulation is due to efflux pumps, or to dysfunctional uptake systems, any of which render in practice the cell resistant to the drug. In such cases, using vectors such as cell-penetrating peptides [CPPs, reviewed in (Koren and Torchilin 2012; MacEwan and Chilkoti 2013; Svensen et al. 2012)] for drug translocation may overcome the resistance, either by impairing cargo detection by ABC transporters (Aroui et al. 2009), or by opening an alternate entry route independent of canonical transporters (Lindgren et al. 2006). CPP-mediated delivery of nucleotides that correct genetic deficiencies (El Andaloussi et al. 2012), of peptides that modulate apoptosis (Boohaker et al. 2012; Li et al. 2011), or of drugs with otherwise poor bioavailability (Choi et al. 2011; Khafagy el and Morishita 2012), have been reported and eventually reached clinical trials (Wang and Wang 2012).

The nature of CPP-cargo linkage, a crucial issue in CPP delivery strategies (Huang et al. 2013; Nasrolahi Shirazi et al. 2013), can be roughly divided into covalent and non-covalent. The latter is preferred for large payloads such as proteins or, especially, nucleic acids (Crombez et al. 2011; Deshayes et al. 2010; Henriques et al. 2005; Lindberg et al. 2013), whose charge complementarity with cationic CPPs is thus usefully exploited. For smaller size cargos like pharmaceuticals, however, low yields of non-covalent complex formation often prevent success. In such cases a covalent approach, where the CPP is either fused with a cargo sequence (Tyagi et al. 2001) or conjugated by various ligation chemistries (Beaudette et al. 2009; Dutot et al. 2009; Steven and Graham 2008), is favored. Reversible strategies relying on disulfide-linked conjugates reductively scissile by cytoplasm redox systems offer distinct advantages in this regard (Barnes and Shen 2009). These CPP-based approaches have been broadly explored for drug delivery to tumor cells, but rarely for infectious disease, where they might serve to face the rising threat of multiresistant pathogens, exacerbated by the dearth of new antibiotic leads in drug pipelines (Coates and Halls 2012).

Miltefosine (MT, hexadecylphosphocholine), originally developed as an antitumoral, finds now a major therapeutic application as the first successful oral drug against leishmaniasis [reviewed in (Dorlo et al. 2012)]. With an annual incidence of nearby 2 million people worldwide, and approximately 50,000 casualties in recent outbreaks in Sudan and Ethiopia, leishmaniasis ranks second only to malaria among protozoan diseases (Alvar et al. 2012) and remains a formidable health challenge. An effective vaccine is proving elusive, and chemotherapy continues to rely on dated, rather toxic antimonials beset by resistance in endemic foci (Chappuis et al. 2007; Rijal et al. 2013). Together with MT, amphotericin B (usually in liposomal formulation) or paromomycin are recent additions to first-line anti-leishmanial agents (den Boer et al. 2009) but limited to combination therapies also threatened by emerging resistance (Garcia-Hernandez et al. 2012). Clearly, novel therapeutic approaches are required to redress such a discouraging scenario.

MT is a good example of an effective drug with non-optimal absorption profile. Upon MT exposure *Leishmania* promastigotes develop a resistant phenotype featuring poor MT accumulation (Perez-Victoria et al. 2003), due to the failure of the sole uptake system known for the parasite, i.e., the aminophospholipid translocase LdMT (*Leishmania donovani* miltefosine transporter) (Seifert et al. 2007) and its regulatory subunit LdRos. As a tool for facilitating MT internalization, hence defeating this MT resistance in *Leishmania*, we have explored the use of Tat(48-60), one of the most representative cell-penetrating peptides (CPPs) (Luque-Ortega et al. 2012).

To monitor the distribution and localization of MT within the parasites, a BODIPY (BDP)-containing analog, adequately functionalized for conjugation to Tat(48-60), was required. Earlier work had determined the optimal location within the MT alkyl chain for a BDP moiety (Hornillos et al. 2006, 2008) in terms of preserving both leishmanicidal activity and recognition by the *Leishmania* uptake system, and also shown that both properties were unaffected by incorporation of an ω-thiol group. These preliminary results inspired the development of MT-BDP-SH (**1**), whose synthesis is described here in detail for the first time. Subsequent conjugation of **1** to Tat(48-60), via either disulfide or thioether bonds, enabled the intracellular delivery of **1** and, for MT-resistant strains, the overcoming of the resistance (Luque-Ortega et al. 2012). The conjugates were mostly built in the solid phase, by judicious choice of protecting groups on two strategic residues (Schemes 1, 3). In addition to the BDP moiety embedded in **1**, the disulfide-based conjugate was labeled at the Tat peptide moiety with Quasar 640, a non-overlapping fluorophore so that redox scission inside the parasite resulted in different fluorescent patterns illustrating the intracellular localization of the MT-like moiety and its Tat vector.

The main advantage of the present approach is the ability to turn into susceptible the hitherto resistant parasite cells and thus overcome the limitations and broaden the therapeutic scope of the drug. In addition, conjugation to Tat enables MT uptake into terminally differentiated cells such as non-infected macrophages, hence expanding the range of MT cellular targets, hitherto limited to tumor cells. This in turn can pave the way for modulating macrophage functionality, a key step towards immune system readjustment, with many possibilities to follow.

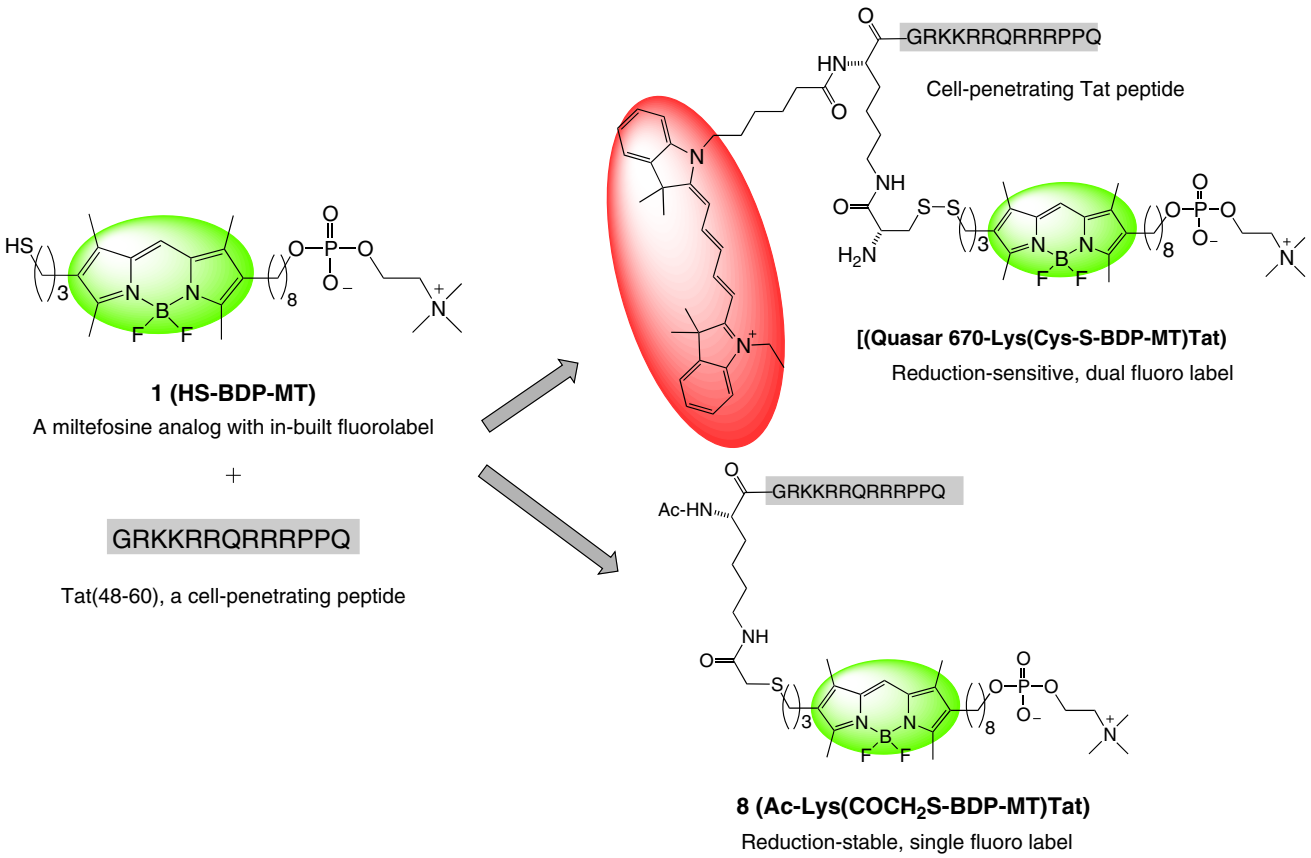

Scheme 1 Synthetic approaches to Tat-linked fluorescent miltefosine derivatives

Materials and methods

HS-BDP-MT (**1**) synthesis

All reactions were carried out under Ar. Commercial reagents were used as received. Solvents were purified by standard methods and deoxygenated thoroughly with Ar bubbling prior to use. Yields refer to the isolated pure compound. Analytical TLC was carried out on Merck 60F 254, 0.25 mm precoated silica gel plates. Flash column chromatography was performed on Merck 60 silica gel, 230–400 mesh, 0.040–0.063 mm. HPLC analyses were done on an Agilent 1100 system equipped with an Eclipse C_{18} reverse phase column (4.6 × 150 mm, 5 µm, Agilent) and a diode array detector. ^{1}H and ^{13}C NMR spectra were recorded on Bruker-300 and Varian 400 spectrometers, respectively. Chemical shifts are reported in parts per million (ppm), using the ^{1}H signal of (trace) chloroform or the ^{13}C signal of $CDCl_3$ (δ 7.26 and 77.0, respectively) as internal references. Abbreviations: s (singlet), d (doublet), t (triplet), q (quartet), m (complex multiplet), b (broad). Assignments are based on COSY, HSQC and HMBC experiments. IR spectra (in cm^{-1}) were recorded on Perkin-Elmer 681 and FT-spectrum one spectrometers. Low-resolution mass spectra were recorded by electron impact (70 eV) in a Hewlett-Packard 5973 spectrometer in the direct injection mode, or by electrospray ionization in a Hewlett-Packard 1100 spectrometer in the positive mode (ESI+). High-resolution mass spectra were registered in an AutoSpec Micromass (Waters) instrument in the L-SIMS mode using Cs+ (30 kV) in m-NBA matrix, with PEG as internal standard. UV–VIS absorption spectra were recorded on Varian CARY-3E or Perkin Elmer Lambda-2 spectrophotometers. Stationary fluorescence excitation and emission spectra were recorded in an ISS PC1 photon counting spectrofluorimeter and corrected for instrumental factors. Relative fluorescence quantum yields were determined, with an uncertainty of 10–20 %, by reference to that of the BODIPY dye PM567, $\Phi_f = 0.91$ in methanol at 20 °C (Saugar et al. 2007).

Synthetic route to **1**

*8-[6′-(3″-Bromopropyl)-1′,3′,5′,7′-tetramethyl-4′,4′-difluoro-4′-bora-3′a,4′a-diaza-s-indacen-2′-yl]octyl trifluoroacetate (**4**) (Scheme 2)*

Phosphorus oxychloride (167 mg, 102 µL, 1.09 mmol) was added under Ar to a stirred solution of pyrroles **2** and **3**

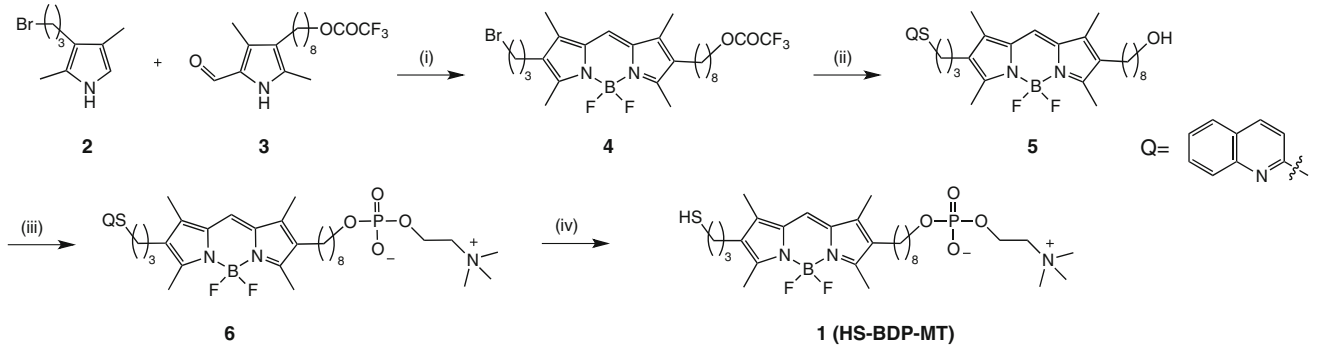

Scheme 2 Reagents and conditions: (i) $POCl_3$, CH_2Cl_2, Ar, 5 h, then DIPEA, $BF_3{\cdot}OEt_2$, 25 min, 85 %; (ii) 2-quinolinethiol, MeONa/MeOH, reflux, 2 h, 95 %; (iii) 2-chloro-1,3,2-dioxaphospholane-2-oxide (2 equiv), Me_3N, MeCN, Ar, pressure tube, −78 °C, then room temp, 3 h, then 80 °C, 4 h, 43 %; (iv) $NaBH_3CN$, HOAc, room temp, 2 h, then H_2O, 1 h, 94 %

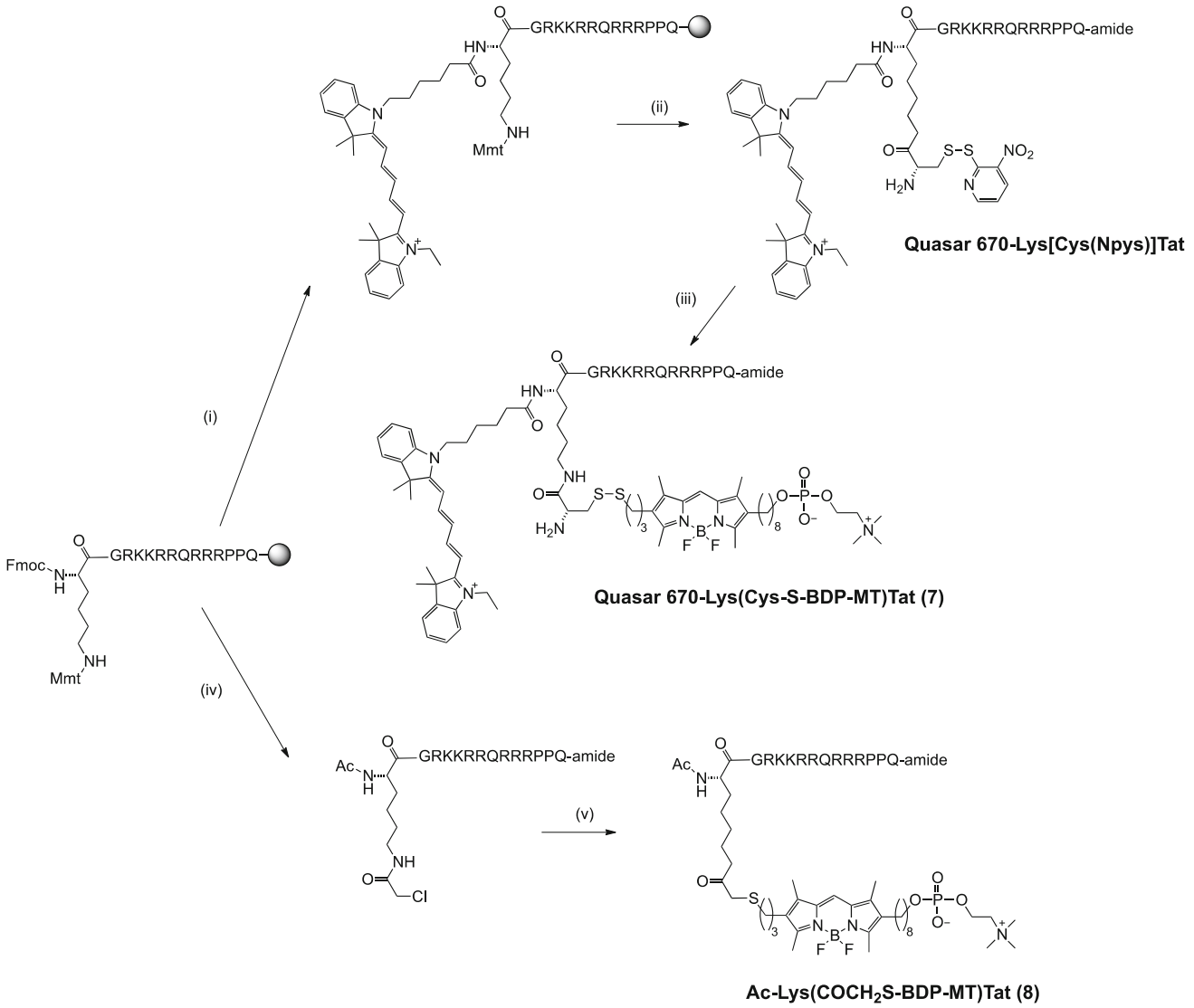

Scheme 3 Reagents and conditions: (i) piperidine/DMF (1:4), 1 + 20 min, then Quasar 670 carboxylic acid, DIPCI (3 equiv), CH_2Cl_2, 1 h; (ii) TFA/CH_2Cl_2, (1 %), then Boc-Cys(Npys)-OH, DIPCI (3 equiv each), CH_2Cl_2, 1 h, then TFA/H_2O/TIS (95:2.5:2.5 v/v), 90 min, HPLC purification; (iii) pH 5, then 1 (1 equiv) in methanol, HPLC purification; (iv) piperidine/DMF (1:4), 1 + 20 min, then Ac_2O/DIEA (2:1) in DMF, 30 min, then TFA/CH_2Cl_2 (1 %), then $ClCH_2COOH$/DIPCI, (5 equiv each), CH_2Cl_2, 1 h, then TFA/H_2O/TIS (95:2.5:2.5 v/v), 90 min, HPLC purification; (v) 20 mM ammonium bicarbonate, pH 7.2, then 1 (1 equiv) in methanol, 30 °C, HPLC purification

(236 and 380 mg, respectively; 1.09 mmol each; see Supporting Information for details on their synthesis) in CH_2Cl_2 (150 mL). After stirring for 5 h at r.t. *N,N*-Diisopropylethylamine (DIEA, 950 μL, 5.45 mmol) and, after 5 min, $BF_3{\cdot}OEt_2$ (685 μL, 5.45 mmol) were added. After 5 min, the same amounts of DIEA and $BF_3{\cdot}OEt_2$ were added again, and the mixture was further stirred for 20 min. After workup, the crude product was purified by column chromatography (silica gel, hexane–EtOAc 9:1). Red solid, yield 725 mg, 85 %. TLC (hexane–EtOAc 4:1): $R_f = 0.60$; ^{1}H NMR (400 MHz, $CDCl_3$, see Supporting Information for carbon numbering): δ 1.26–1.46 (m, 10H, H-3 to H-7), 1.74 (q, $J = 6.9$ Hz, 2H, H-2), 1.99 (q, $J_{obs} = 6.9$ Hz, 2H, H-2″), 2.15, 2.19 (two s, 3H each, CH_3-C1′, CH3-C7′), 2.35 (t, $J = 7.5$ Hz, 2H, H-8), 2.48, 2.49 (two s, 3H each, CH_3-C3′, CH_3-C5′), 2.54 (t, $J = 7.4$ Hz, 2H, H-1″), 3.41 (t, $J = 6.4$ Hz, 2H, H-3″), 4.34 (t, $J = 6.7$ Hz, 2H, H-1), 6.96 (s, 1H, H-8′); ^{13}C NMR (100 MHz, $CDCl_3$): δ 9.6, 9.7 (CH_3-C1′, CH_3-C7′), 12.6, 12.8 (CH_3-C3′, CH_3-C5′), 22.3 (C-1″), 24.0 (C-8), 25.4, 29.0, 29.2, 29.3, 30.0 (C-3 to C-7), 28.0 (C-2), 32.9 (C-2″), 33.2 (C-3″), 68.2 (C-1), 115.9 (CF_3), 118.8 (C-8′), 127.7, 130.6, 132.1, 132.8, 137.1, 137.6 (C-1′, C-2′, C-6′, C-7′, C-7′a, C-8′a), 154.0, 155.9 (C-3′, C-5′), 157.7 (C=O); FT IR (KBr) ν_{max}: 2,930, 2,858, 1,785 ($\nu_{C=O}$), 1,606, 1,473, 1,403, 1,229, 1,065 cm^{-1}; EI MS, *m/z* (%): 592 [M^+] (not observed), 496 (28), 476 (37), 381 [$M^-{\cdot}C_7H_{14}OCOCF_3$] (100).

8-[6′-(3″-Quinol-2‴-ylthiopropyl)-1′,3′,5′,7′-tetramethyl-4′,4′-difluoro-4′-bora-3′a,4′a-diaza-s-indacen-2′-yl]octan-1-ol (5) (Scheme 2)

A previously described method was used (Imahori et al. 2001). Briefly, a solution of 2-quinolinethiol (76 mg, 0.47 mmol) and NaOMe (25 mg, 0.47 mmol) in MeOH (10 mL) was stirred for 30 min at r.t. Compound **4** was then added and the resulting solution was refluxed for 2 h. The solvent was removed under vacuum and the residue was extracted with MeCN (3 × 20 mL), the combined extracts were vacuum evaporated and the residue was purified by column chromatography (silica gel, hexane–EtOAc 7:3). Red solid, yield 65 mg, 95 %. TLC (hexane–EtOAc 1:1): $R_f = 0.50$; ^{1}H NMR (400 MHz, $CDCl_3$, see Supporting Information for carbon numbering): δ 1.27–1.35 (m, 8H, H-3 to H-6), 1.41 (m, 2H, H-7), 1.55 (q, $J = 6.9$ Hz, 2H, H-2), 1.93 (q, $J_{obs} = 7.4$ Hz, 2H, H-2″) 2.14, 2.17 (two s, 3H each, CH_3-C1′, CH_3-C7′), 2.33 (t, $J = 7.5$ Hz, 2H, H-8), 2.48, 2.51 (two s, 3H each, CH_3-C3′, CH_3-C5′), 2.57 (t, $J = 7.6$ Hz, 2H, H-1″), 3.34 (t, $J = 7.3$ Hz, 2H, H-3″), 3.62 (t, $J = 6.6$ Hz, 2H, H-1), 6.93 (s, 1H, H-8′), 7.19 (d, $J = 8.6$ Hz, 1H, H-3‴), 7.42 (m, 1H, H-7‴), 7.63 (m, 1H, H-6‴), 7.70 (dd, $J = 8.1$, 1.0 Hz, 1H, H-8‴), 7.88 (d, $J = 8.7$ Hz, 1H, H-4‴), 7.93 (d, $J = 8.0$ Hz, 1H, H-5‴); ^{13}C NMR (100 MHz, $CDCl_3$): δ 9.5, 9.6 (CH_3-C1′, CH_3-C7′), 12.7, 12.8 (CH_3-C3′, CH_3-C5′), 23.2 (C-1″), 24.0 (C-8), 25.7, 29.2, 29.3, 29.3, 29.4, 29.6. 30.0 (C-3 to C-7, C-2″, C-3″), 32.7 (C-2), 62.9 (C-1), 118.6 (C-8′), 120.9 (C-3‴), 125.2 (C-7‴), 125.8 (C-4‴a), 127.5, 127.8 (C-5‴, C-8‴), 129.7 (C-6‴), 135.4 (C-4‴), 127.7, 130.4, 132.2, 132.5, 137.0, 137.2 (C-1′, C-2′, C-6′, C-7′, C-7′a, C-8′a), 148.0 (C-8‴a), 154.4, 155.3 (C-3′, C-5′), 159.0 (C-2‴); EI MS, *m/z* (%): 577 [M^+] (11), 557 [$M^-{\cdot}$HF] (89), 537 [$M^-{\cdot}(2 \times$ HF)] (100), 396 (63), 370 (40), 301 (95), 273 (65).

*8-[6′-(3′′′-Quinol-2‴-ylthiopropyl)-1′,3′,5′,7′-tetramethyl-4′,4′-difluoro-4′-bora-3′a,4′a-diaza-s-indacen-2′-yl]octylphosphocholine (**6**) (Scheme 2)*

Trimethylamine (ca. 2 mL) was condensed into a solution of alcohol **5** (63 mg, 0.11 mmol) in MeCN (10 mL) in an open pressure tube at −78 °C under Ar. 2-Chloro-1,3,2-dioxaphospholane-2-oxide (20 μL, 0.22 mmol) was then added to the cooled solution and the tube was closed and left 3 h at r.t. and 4 h at 80 °C. After cooling back to r.t. the reactor was opened, the solvent and the unreacted trimethylamine were vacuum evaporated, the residual solid was dissolved in THF-H_2O 9:1 (10 mL), and Amberlite MB-3 was added until resin saturation. The mixture was filtered, the separated solid was washed with MeOH (3 × 10 mL), the filtrate and washings were collected, the solvent was evaporated, and the residual solid was purified by column chromatography (silica gel, first eluting with $CHCl_3$–MeOH 9:1, for the separation of non-polar products, and then with $CHCl_3$–MeOH–H_2O 65:25:5). Red solid, yield 35 mg, 43 %. TLC ($CHCl_3$–MeOH–H_2O 65:25:5): $R_f = 0.40$; ^{1}H NMR (400 MHz, CD_3OD, see Supporting Information for carbon numbering): δ 1.28–1.37 (m, 8H, H-3 to H-6), 1.39 (m, 2H, H-7), 1.62 (q, $J = 6.7$ Hz, 2H, H-2), 1.90 (q, $J_{obs} = 7.4$ Hz, 2H, H-2″), 2.15, 2.16 (two s, 3H each, CH_3-C1′, CH_3-C7′), 2.37 (t, $J = 7.4$ Hz, 2H, H-8), 2.42, 2.43 (two s, 3H each, CH_3-C3′, CH_3-C5′), 2.57 (t, $J = 7.4$ Hz, 2H, H-1′'), 3.19 (s, 9H, N(CH_3)$_3$), 3.29 (t, $J = 7.5$ Hz, 2H, H-3″), 3.59 (m, 2H, CH_2N), 3.86 (td, $J = 6.7$, 6.5 Hz, 2H, H-1), 4.22 (m, 2H, OCH_2CH$_2$N), 7.19 (s, 1H, H-8′), 7.22 (d, $J = 8.7$ Hz, 1H, H-3‴), 7.41 (ddd, $J = 8.1$, 7.0, 1.2 Hz, 1H, H-7‴), 7.60 (ddd, $J = 8.5$, 7.0, 1.5 Hz, 1H, H-6‴), 7.75 (dd, $J = 8.1$, 1.3 Hz, 1H, H-8‴), 7.80 (m, 1H, H-5‴), 7.97 (d, $J = 8.7$ Hz, 1H, H-4‴); ^{13}C NMR (100 MHz, CD_3OD): δ 9.6, 9.7 (CH_3-C1′, CH_3-C7′), 12.9 (CH_3-C3′, CH_3-C5′), 24.0 (C-1″), 24.8 (C-8), 27.0, 30.0, 30.5, 30.5, 30.7, 31.0, 31.3, 31.8, 31.9 (C-2 to C-7, C-2″, C-3″), 54.65, 54.69, 54.72 (N(CH_3)$_3$), 60.3 (d, $J = 4.7$ Hz, OCH_2CH$_2$N), 66.9 (d, $J = 6.1$ Hz, C-1), 67.5 (b s, CH_2N), 120.8 (C-8′), 121.9

(C-3‴), 126.5, 130.9 (C-6‴, C-7‴), 127.4 (C-4‴a), 128.7, 128.9 (C-5‴, C-8‴), 130.2, 131.6, 133.8, 134.0, 139.1, 139.2 (C-1′, C-2′, C-6′, C-7′, C-7a′, C-8′a), 136.9 (C-4‴), 149.5 (C-8‴a), 155.5, 156.1 (C-3′, C-5′), 160.7 (C-2‴); ESI$^+$ MS, *m/z*: 743 [M+H$^+$].

*8-[6′-(3″-Mercaptopropyl)-1′,3′,5′,7′-tetramethyl-4′,4′-difluoro-4′-bora-3a′,4a′-diaza-s-indacen-2′-yl]octyl-phosphocholine (**1**, HS-BDP-MT) (Scheme 2)*

A described deprotection procedure was applied (Nakamura et al. 2002; Zhang and Matteucci 1999). $NaBH_3CN$ (15 mg, 0.236 mmol) was added at r.t. to a solution of **6** (35 mg, 0.047 mmol) in HOAc (0.9 mL), and the mixture was stirred for 2 h. Water (0.7 mL) was then added, and the reaction mixture was further stirred for 1 h. After the subsequent workup, the isolated residue was purified by column chromatography (silica gel, first eluting with $CHCl_3$–MeOH 9:1, for the separation of non-polar products, and then with $CHCl_3$–MeOH–H_2O 65:25:5). Red solid, mp 199–201 °C, yield 27 mg, 94 %. TLC (chloroform–methanol–water 65:25:5): $R_f = 0.40$; ^{1}H NMR (400 MHz, CD_3OD, see Supporting Information for carbon numbering): δ 1.30–1.38 (m, 8H, H-3 to H-6), 1.42 (m, 2H, H-7), 1.64 (q, $J = 6.7$ Hz, 2H, H-2), 1.72 (q, $J_{obs} = 7.3$ Hz, 2H, H-2″), 2.17, 2.18 (two s, 3H each, CH_3-C1′, CH_3-C7′), 2.38 (t, $J = 7.5$ Hz, 2H, H-8), 2.42, 2.43 (two s, 3H each, CH_3-C3′, CH_3-C5′), 2.50 (m, 4H, H-1″, H-3″), 3.22 (s, 9H, N(CH_3)$_3$), 3.63 (m, 2H, CH_2N), 3.87 (td, $J = 6.7$, 6.5 Hz, 2H, H-1), 4.25 (m, 2H, OCH_2CH$_2$N), 7.24 (s, 1H, H-8′); ^{13}C NMR (100 MHz, CD_3OD): δ 9.6 (*C*H$_3$-C1′, *C*H$_3$-C7′), 12.8, 12.9 (*C*H$_3$-C3′, *C*H$_3$-C5′), 23.4, 24.6 (C-1″, C-3″), 24.8 (C-8), 30.4, 30.5, 30.7, 31.3, 31.8, 31.9 (C-2 to C-7), 35.5 (C-2″), 54.68, 54.72, 54.75 (N(*C*H$_3$)$_3$), 60.3 (d, $J = 4.9$ Hz, O*C*H$_2$CH$_2$N), 66.9 (d, $J = 5.9$ Hz, C-1), 67.5 (b s, *C*H$_2$N), 120.8 (C-8′), 130.2, 131.6, 133.8, 134.0, 139.1, 139.2 (C-1′, C-2′, C-6′, C-7′, C-7′a, C-8′a), 155.4, 156.1 (C-3′, C-5′); FT IR (KBr) ν_{max}: 3,435, 2,927, 2,855, 1,606, 1,474, 1,228 ($\nu_{P=O}$), 1,069 (ν_{P-O-C}), 969 cm^{-1}; ESI$^+$ MS, *m/z*: 616 [M + H$^+$], 638 [M + Na$^+$]; HR MS (*peak matching*): calculated for $C_{29}H_{49}BF_2N_3O_4PS$+H 616.3,321; found 616.3,319; HPLC (reverse phase C_{18} column, MeOH–H_2O 9:1, 1.2 mL min^{-1}, λ_{anal} 280, 380 and 503 nm: $R_t = 2.63$ min (100 % purity); UV–VIS (EtOH) λ_{max} (nm) (ε, M^{-1} cm^{-1}): 380 (10,000), 502 (35,000), 529 (82,000); emission (EtOH, corrected): λ_{max} 538 nm; fluorescence quantum yield: 0.70 (10^{-6} M solution in EtOH).

Peptide and conjugate synthesis

Fmoc-protected amino acids, HBTU and Fmoc-Rink-amide resin were from Iris Biotech (Marktredwitz, Germany). HPLC-grade CH_3CN and peptide synthesis-grade DMF, CH_2Cl_2, DIEA and TFA were from Carlo Erba (Sabadell, Spain). All other reagents were of the highest quality commercially available from Sigma-Aldrich (Madrid, Spain). The Tat(48-60) peptide was assembled in an ABI433 peptide synthesizer (Applied Biosystems, Foster City, CA, USA) running Fmoc (FastMoc) SPPS protocols at 0.1 mmol scale. Side chains were protected with Boc (Lys), N^G-2,2,4,6,7-pentamethyldihydrobenzofuran-5-sulfonyl (Arg) and trityl (Gln) groups. The canonic sequence was elongated at the N-terminus with a Lys residue protected at the side chain with the Mmt group. Eightfold excess of Fmoc-L-amino acids and HBTU, in the presence of a double molar amount of DIEA, were used for the coupling steps, with DMF as solvent. Resin-bound peptides were fully deprotected and cleaved by treatment with TFA/H_2O/TIS (95:2.5:2.5 v/v, 90 min. Analytical reversed-phase HPLC was performed on C_{18} columns (4.6 × 50 mm, 3 μm, Phenomenex, Torrance, CA, USA) in a model LC-2010A system (Shimadzu, Kyoto, Japan). Solvent A was 0.045 % (v/v) TFA in water, solvent B was 0.036 % (v/v) TFA in CH_3CN. Elution was done with linear gradients (see Supporting Information) of solvent B into A over 15 min at 1 mL/min flow rate, with UV detection at 220 nm. Preparative HPLC was performed on C_{18} (10 × 250 mm, 10 μm, Phenomenex) in a Shimadzu LC-8A instrument. Solvents A and B were 0.1 % TFA (v/v) in water and CH_3CN, respectively, and elution was again with linear gradients of solvent B into A over 30 min, at 7 mL/min flow rate with UV detection at 220 nm. Fractions of satisfactory purity (>95 %) by analytical HPLC were pooled and lyophilized. Purified peptides and conjugates were characterized for identity by MS as indicated below.

Synthesis of Quasar 670-Lys(Cys-S-BDP-MT)Tat (**7**)

One half of the Fmoc-Lys(Mmt)-elongated Tat peptide-resin (50 μmol) was treated with piperidine/DMF (1:4 v/v, 1 + 20 min) to remove the Fmoc group, then acylated with Quasar 670 (indo-5-carbocyanine *N*-ethyl-*N*′-hexanoic acid; 74 mg, 150 μmol) with DIPCI (23 μL, 150 μmol) activation in CH_2Cl_2 for 1 h. The peptide-resin was treated with 1 % TFA/CH_2Cl_2 to remove the Mmt group, neutralized with 5 % DIEA/CH_2Cl_2 and Boc-Cys(Npys) (53 mg, 150 μmol) was coupled at the Lys ε-amino function, with DIPCI activation (150 μmol) in CH_2Cl_2 for 1 h. Deprotection (except the Npys group) and cleavage of the peptide-resin were done with TFA/H_2O/TIS (95:2.5:2.5 v/v), for 90 min, followed by HPLC purification and lyophilization. Next, the Quasar 670-Lys[Cys(Npys)]Tat peptide (4 mg, 1.6 μmol) was dissolved in 5 mL H_2O, pH was adjusted to 5.0, and 24 μL of a 65 mM solution of **1**

(1.6 μmol) in methanol was added. The reaction mixture was stirred at r.t. until HPLC analysis showed complete conversion to **7**, then diluted with 5 mL H_2O, purified by HPLC and lyophilized to give 2.8 mg of conjugate **7**, amounting to 60 % yield in the disulfide formation and purification steps. **7** was characterized by analytical HPLC and MS (Figs. S3 and S4, Supporting Information).

Synthesis of Ac-Lys($COCH_2$-S-BDP-MT)Tat (**8**)

The other half (50 μmol) of the Fmoc-Lys(Mmt)-elongated Tat peptide-resin was deprotected with piperidine/DMF (1:4, 1 + 20 min), then acetylated with acetic anhydride/DIEA (1:2) in DMF for 1 h. The peptide-resin was next treated with 1 % TFA/CH_2Cl_2 to remove the Mmt group, neutralized with 5 % DIEA/CH_2Cl_2, then chloroaceticacid acid (24 mg, 250 μmol, 5 equiv) was coupled with DIPCI (39 μL, 250 μmol, 5 equiv) activation in CH_2Cl_2 for 1 h. Deprotection and cleavage of the peptide-resin, followed by HPLC purification and lyophilization, were as above. Next, purified Fmoc-Lys(chloroacetyl)Tat (2 mg, 1 μmol) was dissolved in 5 mL of 20 mM ammonium bicarbonate, pH 7.2, and reacted with 32 μL of a 65 mM methanolic solution of **1** (2 μmol), and the reaction mixture was stirred at 30 °C until HPLC analysis showed no further progress. At that point, the reaction was quenched by addition of 5 mL of 10 % HOAc, then purified by HPLC and lyophilized to give 0.9 mg of conjugate **8**, amounting to 35 % yield in the thioether formation and purification steps. **8** was characterized by analytical HPLC and MS (Figs. S5 and S6, Supporting Information).

Parasites and macrophages

Leishmania donovani wild-type (MHOM/ET/67/L82) and MT-resistant (MHOM/ET/67/L82R40, kindly provided by Prof. S. L. Croft; London School of Hygiene and Tropical Medicine) promastigotes were grown at 25 °C in RPMI medium supplemented with 10 % heat-inactivated fetal calf serum, gentamicin, penicillin, and 2 mM glutamine. The R40 MT-resistant phenotype was maintained by adding 40 μM MT to the growth medium. Before each assay, parasites were harvested at late exponential phase and washed twice in Hanks balanced salt solution supplemented with 10 mM D-glucose (pH 7.2) (HBSS-Glc).

Peritoneal macrophages were elicited in 8-week-old Balb/C mice (animal facility, Centro de Investigaciones Biológicas, Madrid) by intra-peritoneal injection of sodium thioglycolate. Three days later macrophages were harvested by peritoneal washing with Hanks buffer and washed in the same medium, then seeded onto 14-mm-diameter circular coverslides (Thermo Scientific, Braunschweig, Germany) as described (Luque-Ortega et al. 2012). Procedures were approved by the animal welfare committee of the center.

Intracellular uptake and distribution of fluorescent MT analogs

Leishmania R40 promastigotes were resuspended at 2×10^7 cells/mL in HBSS-Glc plus Hoechst 3342 (10 μg/mL final concentration). After 1 h, Quasar 670-Lys(Cys-S-BDP-MT)Tat (**7**) and Ac-Lys($COCH_2$-S-BDP-MT)Tat (**8**), were added at 2.5 μM final concentration and fluorescence observed up to 3 h on a TCS-SP2-AOBS-UV ultraspectral confocal microscope (Leica Microsystems, Heidelberg, Germany) without fixation (Luque-Ortega et al. 2012).

BALB/c peritoneal macrophages seeded on circular coverslides (50,000 cells/coverslide) were incubated with conjugate **7** at a final concentration of 4 μM in RPMI-1640 devoid of phenol red, for 1 h at 37 °C. Cells were washed three times with 1 mL of the same medium supplemented with 10 mg/mL of fatty acid-free BSA (Sigma) to remove non-incorporated conjugate, and incubated in the same medium for an additional 2 h to allow redox release of the drug from Tat. Cells were next incubated for 20 min with Hoechst 3422 and observed in a TCS-SP2-AOBS-UV confocal microscope (Leica) without fixation. For Hoechst 3342, BDP and Quasar λ_{exc} and λ_m were 350/460, 488/520 and 644/670 nm, respectively.

Cytotoxicity

To determine parasite viability, R40 promastigotes were resuspended in full growth medium devoid of phenol red at 2×10^6 cells/mL. Tat(48-60), Quasar 670-Lys(Cys-S-BDP-MT)Tat (**7**) and Ac-Lys($COCH_2$-S-BDP-MT)Tat (**8**), dissolved in the same buffer, were added at the corresponding concentrations to the parasite suspension. Parasites were allowed to proliferate for 72 h at 26 °C. Parasite viability was measured by inhibition of 3-(4,5-dimethylthiazol-2-yl)-2,5-diphenyltetrazolium bromide (MTT, 0.5 mg/mL final concentration) reduction (Luque-Ortega et al. 2012). The insoluble formazan product was solubilized with 5 % (w/v) SDS and detected at 600 nm with a Bio-Rad model 640 microplate reader.

Results and discussion

Design and synthesis of HS-BDP-MT (**1**)

Insertion of fluorescent or other reactive groups into linear chain phospholipids may perturb the polarity balance and conformation of the original amphipathic structure; hence impair recognition and transport of the modified

phospholipid at the cell level, with ensuing loss of bioactivity. In the present case our target was an MT analog with a reporter fluorochrome, a distal thiol reacting group and minimal perturbation of the leishmanicidal properties of the original drug. Previous experience on alkylphosphocholine analogs showed that placing a lipophilic BDP group in the alkyl chain, well separated from the essential phosphocholine polar head-group, might led to compounds with antiparasitic properties similar to those of MT (Hornillos et al. 2006, 2008, 2010). We also assumed that a three-methylene spacer between the thiol and the BDP group would suffice to preserve thiol reactivity and facilitate conjugation. These considerations led to HS-BDP-MT (**1**), where the lipophilic part, consisting of 11 methylene spacers and the BDP fluorochrome, is of similar length as the C_{16} chain of MT.

The synthesis of **1** involved four main steps (Scheme 2, see also Supporting Information, Scheme S1 and subsequent text). Non-symmetric BDP **4** was prepared by MacDonald condensation (Wood and Thompson 2007) between α-H-pyrrole **2** and α-formylpyrrole **3**, both substituted at the 4-position with ω-hydroxyalkyl and ω-bromoalkyl residues, respectively, followed by in situ reaction with $BF_3{\cdot}OEt_2$ in the presence of base. Substitution of the bromide in BDP **4** with the sodium salt of 2-quinolinethiol gave the protected thiol **5** with hydrolysis of the trifluoroacetoxy group (Zhang and Matteucci 1999). Next, the phosphocholine head-group was introduced in the terminal alcohol by reaction with 2-chloro-1,3,2-dioxaphospholane-2-oxide in the presence of trimethylamine, yielding **6**. Finally, the thiol protecting group was successfully cleaved off under mild conditions (Nakamura et al. 2002; Zhang and Matteucci 1999) by reduction with sodium cyanoborohydride in acetic acid, without affecting the BDP fluorophore (sensitive to strong acids, bases or hydrogen) or the phosphocholine group. The overall yield of the target compound **1** was 33 %. All spectroscopic data confirmed the molecular structure of **1**. The analog is stable for months at −20 °C in solid form or in ethanol solution, under an inert atmosphere.

Tat conjugates for BDP-MT internalization

For delivery and visualization of the BDP-labeled MT analog **1**, it was linked to the Tat(48-60) CPP by two different strategies (Scheme 1). The common precursor in both approaches, a Tat(48-60) peptide-resin with an additional ε-Mmt protected Lys residue at the N-terminus (Scheme 3), was further elaborated in two different ways. (i) A disulfide-linked version of the Tat conjugate of **1**, Quasar 670-Lys(Cys-S-BDP-MT)-Tat (**7**, Scheme 3, top) displayed an additional labeling of the Tat moiety by Quasar 670, an indocarbocyanine dye that fluoresces in the red region of the visible spectrum ($\lambda_{exc} = 644$ nm; $\lambda_{em} = 670$ nm), similar to Cy^{TM}5. The rationale for the dual labeling was that a redox-scissile conjugate would facilitate visualization and localization of both MT and Tat moieties upon translocation and intracellular reductive cleavage. The orthogonal protection scheme of the Fmoc-Lys(Mmt)-Tat(48-60) peptide-resin enabled selective deprotection and coupling of Quasar 670 at the N-terminal α-amino group, followed by again selective deprotection-elongation at the Lys ε-amino group with a residue of Cys whose thiol function was protected-activated with an Npys group (Bernatowicz et al. 1986; Mezö et al. 2000; Ridge et al. 1982) to allow subsequent disulfide formation. The resulting Quasar 670-Lys[Cys(Npys)]Tat peptide intermediate was obtained upon acid deprotection/cleavage of the peptide-resin, purified by HPLC, then chemoselectively reacted with thiol **1** in a mildly acidic water–methanol medium where heterodisulfide **7** formation (60 % yield after purification) prevailed upon thiol **1** oxidation/dimerization. (ii) In similar fashion, a thioether version of the conjugate also used Fmoc-Lys(Mmt)-Tat(48-60)-resin as precursor. A simpler labeling scheme with **1** as single fluorochrome was chosen in this case, as the reductively non-scissile nature of thioether **8** made dual labeling superfluous. Thus, the peptide-resin was capped with an Ac group at the N-terminal α-amino group, and the Lys ε-amino group was then elongated with a chloroacetyl (ClAc) group. TFA acidolysis gave a Fmoc-Lys(ClAc)-Tat(48-60) intermediate that, after HPLC purification, underwent nucleophilic substitution by thiol **1** to give Ac-Lys($COCH_2$S-BDP-MT)Tat (**8**). The yield of thioether formation (35 % after purification) was lower than for **7**, reflecting the limited selectivity of the reaction, where substitution competes with thiol dimerization and with Cl displacement in the ClAc group by hydroxyl from the solvent (Monso et al. 2012).

Tat-mediated delivery of MT into *Leishmania* and macrophages

A thorough evaluation of the intracellular delivery of BDP-MT into *Leishmania* by conjugates **7** and **8** has been reported elsewhere (Luque-Ortega et al. 2012) and is only recapped here. First, a cytotoxic effect of **7** and **8** on both promastigote (Fig. 1) and macrophage-infecting amastigote forms of the MT-resistant R40 strain of *L. donovani* was verified, proving the intracellular delivery of BDP-MT, hence the reversal of the resistant condition of the parasites. Second, **7** and **8** were both internalized to a similar extent regardless of disulfide or thioether linkage between Tat and BDP-MT (Scheme 1; Fig. 1). Sagan et al. have shown that disulfide exchange reactions with cell surface thiols can hamper the entry of disulfide-bearing CPPs

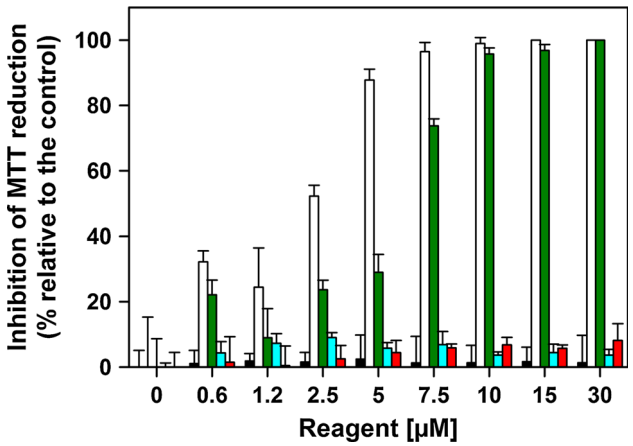

Fig. 1 Tat conjugation overcomes MT resistance in R40 *L. donovani* promastigotes. Inhibition of R40 proliferation by compound **1** (*black bars*), conjugate **7** (*empty bars*), conjugate **8** (*green bars*), Tat(48-60) (*blue bars*) and Tat(48-60)+**1** (1:1 molar ratio, *red bars*) (colour figure online)

(Aubry et al. 2009). Any concerns about conjugate **7** in this regard were not verified; indeed, its uptake in intact form was also indirectly demonstrated by the segregate localization—evidencing post-uptake reductive release—of selectively labeled BDP-MT and Quasar 670-Tat moieties after incubation for 3 h (Fig. 2). Third, the efficient internalization of thioether-linked **8** also showed that a scissile BDP-MT moiety is not mandatory for leishmanicidal activity (Fig. 1).

In *Leishmania*-infected macrophages, MT accumulates mainly in intracellular parasites, hence accounting for leishmanicidal activity, while uptake in the cytoplasm is much lower (Luque-Ortega et al. 2012). For non-infected macrophages, despite their usually high endocytic rates, MT (**1**) uptake is also poor (Fig. 3, lower panels). It seemed thus reasonable to investigate whether Tat conjugation as in **7** and **8** might promote uptake even in the absence of parasite infection. Indeed, when Tat-bound as in **7**, BDP-MT showed outstanding incorporation (Fig. 3, upper panels). Also, areas of predominantly green (BDP-MT) or red (Quasar-Tat) fluorescence could be distinguished, accounting as in the *Leishmania* case for reductive cleavage of the conjugate followed by distribution of the resulting moieties in the macrophage cytoplasm. This strongly suggested that Tat-mediated uptake can expand the range of MT targets to include non-transformed cell types.

For *Leishmania*, amastigote survival and replication within the macrophage are known to rely on activation of various host cell survival pathways upon parasite infection, PI3K/Akt being one of the most notorious (Ruhland et al. 2007). This kinase, in turn, is inhibited by alkyl-lysophospholipids, [reviewed in (van

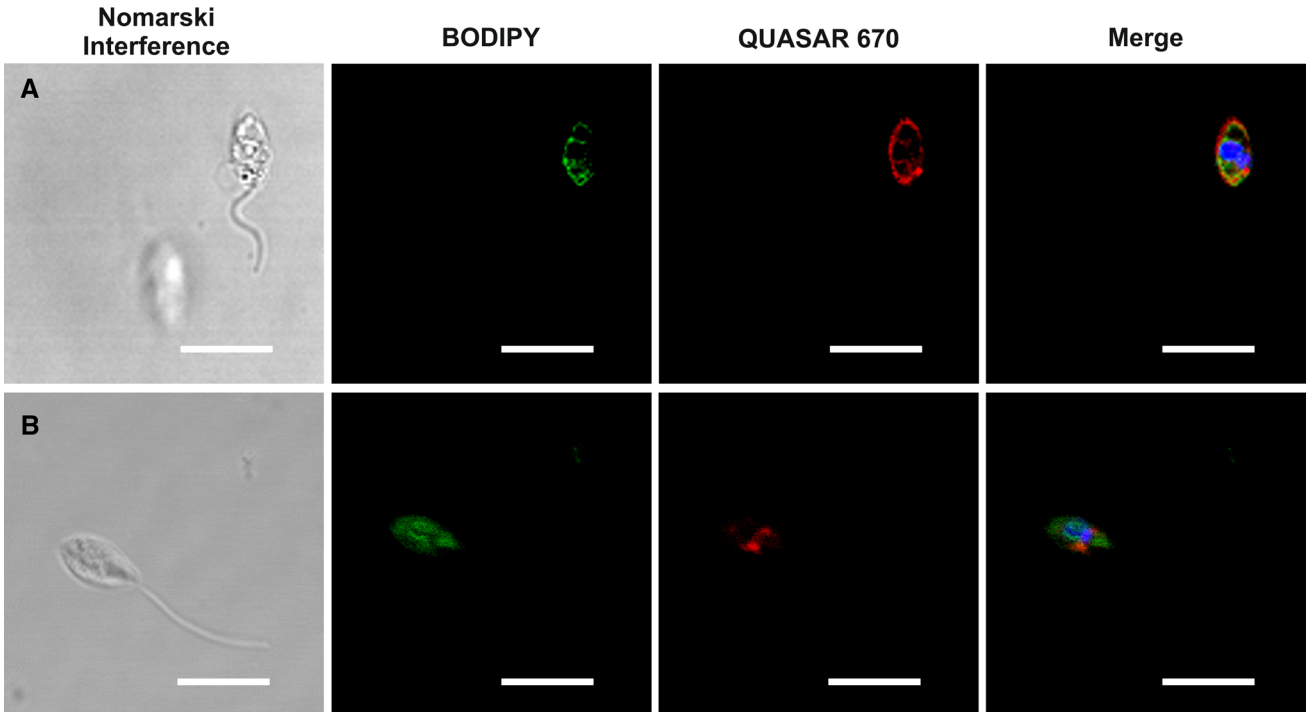

Fig. 2 Intracellular distribution of conjugate **7** in *L. donovani* R40 parasites. Cells were pre-stained with Hoechst 3342 and incubated with 2.5 μM conjugate for 5 min (**a**) or 3 h (**b**), then observed unfixed by confocal microscopy. λ_{exc} and λ_{em} were 350/460 nm for Hoechst 3342; 488/520 nm for BDP and 644/670 for Quasar 670. *Bar* 10 μm

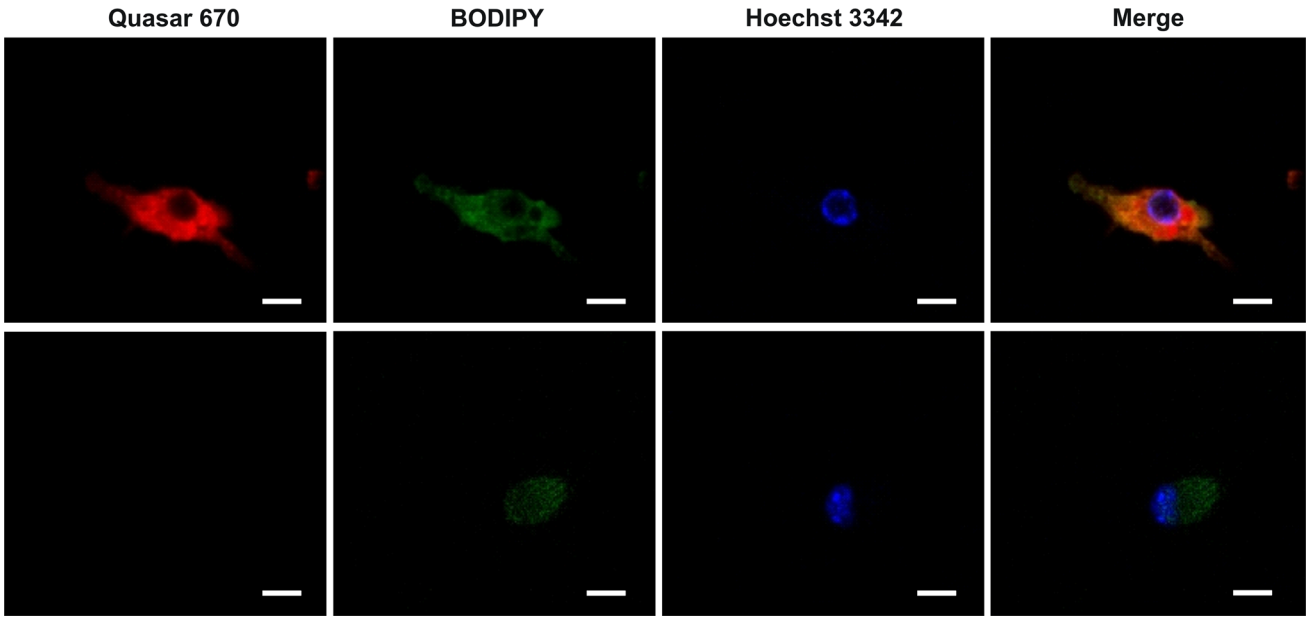

Fig. 3 Effect of Tat conjugation on BDP-MT internalization in macrophages. Balb/C mice peritoneal macrophages were treated with either conjugate 7 (*upper panels*) or non-conjugated 1 (*lower panels*) at 4 μM. Cells were incubated at 37 °C for 1 h, washed and incubated for an additional 2 h. 20 min prior to observation, Hoechst 3342 (10 μg/mL) was added to localize the nucleus. λ_{exc} and λ_{em} were 644/670 for Quasar 670, 488/520 nm for BDP and 350/460 nm for Hoechst 3342. *Bar* 10 μm

Blitterswijk and Verheij 2013)] which as we have just seen can only be efficiently internalized by conjugation to a CPP. Hence, Tat-mediated MT delivery opens up new possibilities of tackling parasitic diseases such as leishmaniasis by modulation of host cell uptake preferences instead of straightforward action on the parasite. In this context, an obvious hurdle is to ensure specific drug action by equally specific MT delivery to a particular cell type target. For macrophages, this could be solved by conjugate encapsulation, taking advantage of the high endocytic rate of these cells. For other cell types, alternative strategies are envisaged such as CPPs with variable degrees of cell selectivity, or standard CPPs endowed with homing peptide sequences that bias conjugate distribution into specific cell types [reviewed in (Svensen et al. 2012)].

Concluding remarks

This work addresses two important issues in drug delivery: (i) the need for fluorescent versions of useful pharmaceuticals, to monitor their cell uptake and distribution, and (ii) expanding the spectrum of cell types susceptible to a given drug. MT, the subject of our study, posed an additional requirement for minimal structural alteration to ensure that antiparasitic action was preserved.

The first issue has been solved by means of HS-BDP-MT (**1**), an analog with an embedded BDP group conferring the desired fluorescent properties, and a thiol group enabling conjugation. The intrinsic structural features of **1** prevented the use of FRET or other strategies to visualize the intracellular splitting of the BDP-MT and Tat moieties of the disulfide conjugate and their resulting subcellular distribution. However, an additional, non-overlapping fluorochrome placed on the Tat peptide successfully allowed to track the cleavage.

As to the second issue, the present work is to our best knowledge the first example of MT conjugation to a CPP, with the ensuing expansion in the range of susceptible cells, so far confined to tumoral phenotypes and lower eukaryotes. Our results with mouse macrophages, serving not only as primary cell models but most importantly as host cells that undergo extensive functional retooling by *Leishmania*, provide the required proof of mechanism and suggest several potential application strategies: (i) treating simultaneously MT targets in both the parasite and the host cell; (ii) treating *Leishmania*-specific targets which the parasite secretes into the macrophage; delivering drugs against these targets through the macrophage—a professional phagocyte—membrane is arguably easier than through the sturdy *Leishmania* membrane; (iii) extrapolation to other macrophage intracellular pathogens such as *Mycobacterium* or *Legionella* with high impact on human health.

Acknowledgments Research supported by funds from the European Union (HEALTH-2007-223414 to L.R. and D.A.),VI PN de I+D+I 2008-2011, (PI09-01928, PI12-02706) and ISCIII-Subdirección

General de Redes y Centros de Investigación Cooperativa (RICET RD 06/0021/0006, RD12/0018/0007 to L.R.) MICINN (CTQ2010-16457 to A.U.A, BIO2008-04487-CO3 to D.A.), MINECO (SAF2011-24899 to D.A.) and Generalitat de Catalunya (SGR2009-00492 to D.A.).

Conflict of interest The authors declare that they have no conflict of interest.

References

Alvar J, Velez ID, Bern C, Herrero M, Desjeux P, Cano J, Jannin J, den Boer M (2012) Leishmaniasis worldwide and global estimates of its incidence. PLoS One 7:e35671

Aroui S, Brahim S, Hamelin J, De Waard M, Breard J, Kenani A (2009) Conjugation of doxorubicin to cell penetrating peptides sensitizes human breast MDA-MB 231 cancer cells to endogenous TRAIL-induced apoptosis. Apoptosis 14:1352–1365

Aubry S, Burlina F, Dupont E, Delaroche D, Joliot A, Lavielle S, Chassaing G, Sagan S (2009) Cell-surface thiols affect cell entry of disulfide-conjugated peptides. FASEB J 23:2956–2967

Barnes MP, Shen WC (2009) Disulfide and thioether linked cytochrome c-oligoarginine conjugates in HeLa cells. Int J Pharm 369:79–84

Beaudette TT, Cohen JA, Bachelder EM, Broaders KE, Cohen JL, Engleman EG, Frechet JM (2009) Chemoselective ligation in the functionalization of polysaccharide-based particles. J Am Chem Soc 131:10360–10361

Bernatowicz MS, Matsueda R, Matsueda GR (1986) Preparation of Boc-[S-(3-nitro-2-pyridinesulfenyl)]-cysteine and its use for unsymmetrical disulfide bond formation. Int J Pept Protein Res 28:107–112

Boohaker RJ, Lee MW, Vishnubhotla P, Perez JM, Khaled AR (2012) The use of therapeutic peptides to target and to kill cancer cells. Curr Med Chem 19:3794–3804

Chappuis F, Sundar S, Hailu A, Ghalib H, Rijal S, Peeling RW, Alvar J, Boelaert M (2007) Visceral leishmaniasis: what are the needs for diagnosis, treatment and control? Nat Rev Microbiol 5:873–882

Choi YS, Lee JY, Suh JS, Lee SJ, Yang VC, Chung CP, Park YJ (2011) Cell penetrating peptides for tumor targeting. Curr Pharm Biotechnol 12:1166–1182

Coates AR Halls G (2012) Antibiotics in phase II and III clinical trials. Handb Exp Pharmacol, 167–183

Crombez L, Morris MC, Heitz F, Divita G (2011) A non-covalent peptide-based strategy for ex vivo and in vivo oligonucleotide delivery. Methods Mol Biol 764:59–73

den Boer ML, Alvar J, Davidson RN, Ritmeijer K, Balasegaram M (2009) Developments in the treatment of visceral leishmaniasis. Expert Opin Emerg Drugs 14:395–410

Deshayes S, Konate K, Aldrian G, Crombez L, Heitz F, Divita G (2010) Structural polymorphism of non-covalent peptide-based delivery systems: highway to cellular uptake. Biochim Biophys Acta 1798:2304–2314

Dorlo TP, Balasegaram M, Beijnen JH, de Vries PJ (2012) Miltefosine: a review of its pharmacology and therapeutic efficacy in the treatment of leishmaniasis. J Antimicrob Chemother 67:2576–2597

Dutot L, Lecorche P, Burlina F, Marquant R, Point V, Sagan S, Chassaing G, Mallet JM, Lavielle S (2009) Glycosylated cell-penetrating peptides and their conjugates to a proapoptotic peptide: preparation by click chemistry and cell viability studies. J Chem Biol 3:51–65

El Andaloussi SA, Hammond SM, Mager I, Wood MJ (2012) Use of cell-penetrating-peptides in oligonucleotide splice switching therapy. Curr Gene Ther 12:161–178

Garcia-Hernandez R, Manzano JI, Castanys S, Gamarro F (2012) *Leishmania donovani* develops resistance to drug combinations. PLoS Negl Trop Dis 6:e1974

Henriques ST, Costa J, Castanho MA (2005) Translocation of beta-galactosidase mediated by the cell-penetrating peptide pep-1 into lipid vesicles and human HeLa cells is driven by membrane electrostatic potential. Biochemistry 44:10189–10198

Hornillos V, Saugar JM, de la Torre BG, Andreu D, Rivas L, Acuna AU, Amat-Guerri F (2006) Synthesis of 16-mercaptohexadecylphosphocholine, a miltefosine analog with leishmanicidal activity. Bioorg Med Chem Lett 16:5190–5193

Hornillos V, Carrillo E, Rivas L, Amat-Guerri F, Acuna AU (2008) Synthesis of BODIPY-labeled alkylphosphocholines with leishmanicidal activity, as fluorescent analogues of miltefosine. Bioorg Med Chem Lett 18:6336–6339

Hornillos V, Tormo L, Amat-Guerri F, Acuña AU (2010) Synthesis and spectral properties of fluorescent linear alkylphosphocholines labeled with all-(E)-1,6-diphenyl-1,3,5-hexatriene. J Photochem Photobiol A 216:79–84

Huang Y, Jiang Y, Wang H, Wang J, Shin MC, Byun Y, He H, Liang Y, Yang VC (2013) Curb challenges of the "Trojan Horse" approach: Smart strategies in achieving effective yet safe cell-penetrating peptide-based drug delivery. Adv Drug Deliv Rev 65:1299–1315

Imahori H, Norieda H, Yamada H, Nishimura Y, Yamazaki I, Sakata Y, Fukuzumi S (2001) Light-harvesting and photocurrent generation by gold electrodes modified with mixed self-assembled monolayers of boron-dipyrrin and ferrocene-porphyrin-fullerene triad. J Am Chem Soc 123:100–110

Khafagy el S, Morishita M (2012) Oral biodrug delivery using cell-penetrating peptide. Adv Drug Deliv Rev 64:531–539

Koren E, Torchilin VP (2012) Cell-penetrating peptides: breaking through to the other side. Trends Mol Med 18:385–393

Li H, Nelson CE, Evans BC, Duvall CL (2011) Delivery of intracellular-acting biologics in pro-apoptotic therapies. Curr Pharm Des 17:293–319

Lindberg S, Munoz-Alarcon A, Helmfors H, Mosqueira D, Gyllborg D, Tudoran O, Langel U (2013) PepFect15, a novel endosomolytic cell-penetrating peptide for oligonucleotide delivery via scavenger receptors. Int J Pharm 441:242–247

Lindgren M, Rosenthal-Aizman K, Saar K, Eiriksdottir E, Jiang Y, Sassian M, Ostlund P, Hallbrink M, Langel U (2006) Overcoming methotrexate resistance in breast cancer tumour cells by the use of a new cell-penetrating peptide. Biochem Pharmacol 71:416–425

Luque-Ortega JR, de la Torre BG, Hornillos V, Bart JM, Rueda C, Navarro M, Amat-Guerri F, Acuna AU, Andreu D, Rivas L (2012) Defeating Leishmania resistance to miltefosine (hexadecylphosphocholine) by peptide-mediated drug smuggling: a proof of mechanism for trypanosomatid chemotherapy. J Control Release 161:835–842

MacEwan SR, Chilkoti A (2013) Harnessing the power of cell-penetrating peptides: activatable carriers for targeting systemic delivery of cancer therapeutics and imaging agents. Wiley Interdiscip Rev Nanomed Nanobiotechnol 5:31–48

Martinez MN, Amidon GL (2002) A mechanistic approach to understanding the factors affecting drug absorption: a review of fundamentals. J Clin Pharmacol 42:620–643

Mezö G, Mihala N, Andreu D, Hudecz F (2000) Conjugation of epitope peptides with SH group to branched chain polymeric polypeptides via Cys(Npys). Bioconjug Chem 11:484–491

Monso M, Kowalczyk W, Andreu D, de la Torre BG (2012) Reverse thioether ligation route to multimeric peptide antigens. Org Biomol Chem 10:3116–3121

Nakamura S, Furutani A, Toru T (2002) Highly enantioselective reaction of α-lithio 2-quinolyl sulfide using chiral bis(oxazoline)s: a new synthesis of enantioenriched thiols. Eur J Org Chem 1690–1695

Nasrolahi Shirazi A, Tiwari R, Chhikara BS, Mandal D, Parang K (2013) Design and biological evaluation of cell-penetrating peptide-doxorubicin conjugates as prodrugs. Mol Pharm 10:488–499

Perez-Victoria FJ, Gamarro F, Ouellette M, Castanys S (2003) Functional cloning of the miltefosine transporter. A novel P-type phospholipid translocase from *Leishmania* involved in drug resistance. J Biol Chem 278:49965–49971

Ridge RJ, Matsueda GR, Haber E, Matsueda R (1982) Sulfur protection with the 3-nitro-2-pyridine sulfenyl group in solid-phase peptide synthesis. Int J Pept Protein Res 19:490–498

Rijal S, Ostyn B, Uranw S, Rai K, Bhattarai NR, Dorlo TP, Beijnen JH, Vanaerschot M, Decuypere S, Dhakal SS, Das ML, Karki P, Singh R, Boelaert M, Dujardin JC (2013) Increasing failure of miltefosine in the treatment of Kala-azar in Nepal and the potential role of parasite drug resistance, reinfection, or noncompliance. Clin Infect Dis 56:1530–1538

Ruhland A, Leal N, Kima PE (2007) Leishmania promastigotes activate PI3K/Akt signalling to confer host cell resistance to apoptosis. Cell Microbiol 9:84–96

Saugar JM, Delgado J, Hornillos V, Luque-Ortega JR, Amat-Guerri F, Acuna AU, Rivas L (2007) Synthesis and biological evaluation of fluorescent leishmanicidal analogues of hexadecylphosphocholine (miltefosine) as probes of antiparasite mechanisms. J Med Chem 50:5994–6003

Seifert K, Perez-Victoria FJ, Stettler M, Sanchez-Canete MP, Castanys S, Gamarro F, Croft SL (2007) Inactivation of the miltefosine transporter, LdMT, causes miltefosine resistance that is conferred to the amastigote stage of *Leishmania donovani* and persists in vivo. Int J Antimicrob Agents 30:229–235

Steven V, Graham D (2008) Oligonucleotide conjugation to a cell-penetrating (TAT) peptide by Diels-Alder cycloaddition. Org Biomol Chem 6:3781–3787

Svensen N, Walton JG, Bradley M (2012) Peptides for cell-selective drug delivery. Trends Pharmacol Sci 33:186–192

Tyagi M, Rusnati M, Presta M, Giacca M (2001) Internalization of HIV-1 tat requires cell surface heparan sulfate proteoglycans. J Biol Chem 276:3254–3261

van Blitterswijk WJ, Verheij M (2013) Anticancer mechanisms and clinical application of alkyl phospholipids. Biochim Biophys Acta 1831:663–674

Wang HY, Wang RF (2012) Enhancing cancer immunotherapy by intracellular delivery of cell-penetrating peptides and stimulation of pattern-recognition receptor signaling. Adv Immunol 114:151–176

Wood TE, Thompson A (2007) Advances in the chemistry of dipyrrins and their complexes. Chem Rev 107:1831–1861

Zhang J, Matteucci MD (1999) A novel thiol protecting group: a 2-thioquinoline sulfide as a masked sulfhydryl moiety. Tetrahedron Lett 40:1467–1470